A determination of the photon PDF from LHC high-mass Drell Yan data

The xFitter Collaboration: F. Giuli, V. Bertone, A. Cooper-Sarkar,
A. Glazov, R. Placakyte, V. Radescu, J. Rojo, A. Sapronov, et al
(Dated: November 30, 2016)

The calculation of electroweak corrections to LHC processes requires by consistency introducing a photon parton distributuon in the proton. In this work we present a determination of the photon PDF from recent ATLAS measurements of high-mass Drell-Yan production at $\sqrt{s} = 8$ TeV. The analysis is performed in the `xFitter` framework. We compare our results with recent calculations of the photon PDF as well as with previous fits, finding good agreement within uncertainties.

CONTENTS

I. INTRODUCTION

Precision phenomenology at the LHC requires theoretical calculations which include not only QCD corrections (where NNLO is rapidly becoming the standard) but also electroweak (EWK) corrections, which become specially relevant for observables directly sensitive to the TeV region. An important ingredient of these electroweak corrections is the photon parton distribution function (PDFs), which must be introduced to regularise the collinear divergences in initial-state QED emissions.

The first PDF fit to include both QED corrections and a photon PDF was MRST2004QED, where the photon PDF was taken from a model and tested on HERA data for direct photon production. More recently, the NNPDF2.3QED set provided a model-independent determination of the photon PDF based on Drell-Yan data from ATLAS and LHCb. The resulting photon PDF is however affected by large uncertainties due to the limited sensitivity of the data used as input to that fit. The CT group have also released a QED fit using a similar strategy as the MRST2004QED one.

A recent breakthrough concerning the determination of the photon PDF has been the realization that it can be expressed in terms of inclusive lepton-proton deep-inelastic scattering structure functions. The residual uncertainties in the photon PDF resulting from this strategy, dubbed LUXqed, are now at the few percent level, not unlike the quark and gluon PDFs. A related approach by the HMR group also leads to a similar photon PDF.

The aim of this work is to perform a direct determination of the photon PDF from the recent high-mass Drell-Yan measurements from the ATLAS experiment at $\sqrt{s} = 8$ TeV, and compare with the various existing calculations. As compared to previous measurements of the Drell-Yan processes at high dilepton invariant masses m_{ll}, ATLAS now provides both single differential distributions in m_{ll} as well as double-differential cross-sections in both m_{ll} and $|y_{ll}|$, the rapidity of the lepton pair, and in m_{ll} and $\Delta\eta_{ll}$, the difference in pseudo-rapidity between the two leptons.

These more differential distributions provide an additional handle on the photon PDF, and indeed it was demonstrated in by means of the Bayesian reweighting method that a significant reduction of the photon PDF uncertainties of NNPDF2.3QED could be achieved following the inclusion of the ATLAS data. The goal of this study is to investigate further these constraints from the ATLAS high-mass measurements on the photon PDF, this time by means of a direct PDF fit performed within the open-source `xFitter` framework. State-of-the-art theoretical calculations will be employed, in particular we include NNLO QCD and NLO QED corrections, the latter implemented via the `APFEL` program and presented from the first time here. Our results turn out to be in good agreement with the LUXqed and HMR calculations, providing further evidence that our understanding of the photon PDF has been significantly improved in the last few months, both from the point of theory and from the point of data.

The outline of this paper is as follows. First of all in Sect. II we present the theoretical calculation of DIS structure functions and of Drell-Yan cross-sections used in this work. Then in Sect III we discuss the settings of the PDF fit, including the parametrization of the photon PDF that will be adopted. Here we also show a sensitivity study which motivates the usefulness of the ATLAS measurements for the photon PDF. The results of this work are presented in Sect. IV, where we also compare with existing calculations and other fits of the photon PDF. Finally in Sect. V we conclude and outline possible future lines of investigation. In addition, appendix A contains a detailed description of the implementation and validation of NLO QED corrections in `APFEL`.

II. THEORY

Two processes contribute to opposite sign, same family, dilepton production at the LHC: the Drell-Yan quark-antiquark process and the photon-induced process. Both the contributions can be simulated with MadGraph5_aMC@NLO (version 2.4.3) and interfaced to APPLgrid (version 01-04-70) and aMCfast (version 01-03-00). A special release of APPLgrid is used to account for the photon PDF within the proton *need references for the programmes*. Both contributions are generated in the 5-flavour scheme, where all the quarks, except for the *top* quark, are treated as massless quarks; all the calculations are performed at fixed-order (FO) without parton showers.

Theoretical predictions for both the one-dimensional $\frac{d\sigma}{dm_{ll}}$ distribution (where m_{ll} is the invariant mass of the dilepton pair in the final state) and the double-differential distributions $\frac{d^2\sigma}{dm_{ll}d|y_{ll}|}$ (where $|y_{ll}|$ is the rapidity of the dilepton pair) and $\frac{d^2\sigma}{dm_{ll}\Delta\eta_{ll}}$ (where $\Delta\eta_{ll}$ represents the difference in pseudorapidity between the two leptons) are generated for both the electron and the muon channels.

These predictions are generated using the same selections as in reference [**?**] as follows:

- the invariant mass of the lepton pair is required to be greater than 116 GeV;
- the absolute value of the pseudorapidity of each lepton is required to be less than 2.5;
- the transverse momentum (p_T) of the leading lepton has to be greater than 40 GeV;
- the p_T of the sub-leading lepton has to be greater than 30 GeV.

The binning used is the same as used in reference [**?**]. For the invariant mass distribution, there are 12 bins between 116 GeV and 1.5 TeV with variable bin widths; and for both of the the two-dimensional distributions, there are five different histograms, each one for a different invariant mass range: (a) 116 GeV $< m_{ll} <$ 150 GeV; (b) 150 GeV $< m_{ll} <$ 200 GeV; (c) 200 GeV $< m_{ll} <$ 300 GeV; (d) 300 GeV $< m_{ll} <$ 500 GeV; (e) 500 GeV $< m_{ll} <$ 1500 GeV. The APPLgrids for the first three m_{ll} intervals are divided into 12 bins with fixed bin width between $|y_{ll}^{mim}|$ ($|\Delta\eta_{ll}|$) = 0.0 (0.0) and $|y_{ll}^{max}|$ ($|\Delta\eta_{ll}|$) = 2.4 (3.0), while the final two m_{ll} intervals are divided into 6 bins with fixed bin width scanning the same $|y_{ll}|$ and $|\Delta\eta_{ll}|$ ranges.

Dynamical renormalization (μ_R) and factorization (μ_R) scales are used in the calculations and both are set to m_{ll}. The theoretical calculations were validated by comparing both the NLO QCD + LO EW predictions and the LO PI predictions to those computed using the FEWZ 3.1 framework. These calculations are evaluated in the G_F electroweak scheme, with the following values for the couplings: $\alpha_S = 0.118$; $1/\alpha_{EW} = 1/127$. The difference between the two predictions is at most 1%, for both the 1-dimensional and the 2-dimensional distributions.

In order to make a next-to-next-to-leading order (NNLO) fit k-factors (k_F) are computed matching the NLO QCD + LO EW cross sections to higher order (HO) calculations. These are computed using FEWZ, with the same input parameters as for the NLO computations. The k_F are defined as:

$$k_F = \frac{NNLO\ QCD + NLO\ EW\sigma}{NLO\ QCD + LO\ EW\sigma} \quad (1)$$

The MMHT2014NNLO PDF set is used to compute both numerator and denominator. The k_F are close to the unity and their variation is $\sim 2\%$. *provide Table of Final k-factors?*

Discuss theory improvements: addition of the NLO QED+QCD piece

III. SETTINGS

In this section we discuss the settings of the PDF fit, including the parametrization of the photon PDF that will be adopted.

IV. RESULTS

A. Sensitivity

show impact of HM DY on PDFs using sensitivity studies based on pseudo-data, for which we only use the data uncertainties, while central value are fixed: HERA I+II vs HERA I+II + HMDY –> see the sensitivity plots from the previous email

conclusion: HMDY data has a large impact on photonPDF

B. PDF Fits

In order to make a full PDF fit the ATLAS Drell-Yan data data are fitted together with the final combined inclusive cross section data from HERA [**?**]. The HERA data provide information on the quark/antiquark and gluon content of the proton and the Drell-Yan data add information on the photon content of the proton. The NLO and NNLO pQCD predictions are fitted to the data using the xFitter open source pQCD fitting platform [**?**]. The DGLAP equations [**?**] are solved using the programme QCDNUM which has been modified to include the photon PDF in the proton [**?**]. The DGLAP equations yield the PDFs at all scales if they are input as finctions of x at a starting scale Q_0^2, which should be large enough that perturbative QCD can be assumed to be valid. For the present analysis this value is chosen to be $Q_0^2 = 7.5$ GeV^2. This is also the value chosen for the

minimum value of Q^2 for data entering the fit. The charm and beauty masses are chosen to be $m_c = 1.47$ GeV and $m_b = 4.5$ GeV following the HERA analysis. The value of $\alpha_s(M_Z)$ is chosen to be $\alpha_s(M_Z) = 0.118$ [**?**]. The value of Q_0^2 is above the charm mass squared, however a version of the programme is used which displaces the charm threshold from the charm mass [**?**] such that the threshold is at Q_0^2. The form of the χ^2 used for the fit is that defined in the H1 paper [**?**]. Alternative forms have also been tried with no significant difference to our results.

The PDF parametrisation input at Q_0^2 is determined by the technique of saturation of the χ^2 [**?**]. The parametrised PDFs are the valence distributions xu_v and xd_v, the gluon distribution xg, and the u-type and d-type sea, $x\bar{U}$, $x\bar{D}$, where $x\bar{U} = x\bar{u}$ and $x\bar{D} = x\bar{d} + x\bar{s}$, and finally the photon distribution $x\gamma$. The following standard functional form is used to parametrise them:

$$xf(x) = Ax^B(1-x)^C(1 + Dx + Ex^2) \tag{2}$$

where the normalisation parameters A_{u_v}, A_{d_v} and A_g are constrained by the number sum-rules and the momentum sum-rule, respectively. The B parameters $B_{\bar{U}}$ and $B_{\bar{D}}$ are set equal, such that there is a single B parameter for the sea distribution. The data are not sensitive to the strangeness content of the proton which is thus set such that $x\bar{s} = 0.5\bar{D}$, following the ATLAS analysis [**?**]. The further constraint $A_{\bar{U}} = 0.5A_{\bar{D}}$ is imposed such that $\bar{u} = x\bar{d}$ as $x \to 0$. The D and E parameters are introduced one by one until no significant improvement in χ^2 is found.

For the NNLO fit a $\chi^2/ndf = 1.18$, with a partial $\chi^2/ndp = 1.15$ for the high-mass Drell-yan data [*update with final numbers*], is achieved for the following parametrisation, which has 11 parameters for the quarks and gluons and 5 parameters for the photon:

$$xu_v(x) = A_{u_v}x^{B_{u_v}}(1-x)^{C_{u_v}}(1 + E_{u_v}x^2), \tag{3}$$
$$xd_v(x) = A_{d_v}x^{B_{d_v}}(1-x)^{C_{d_v}}, \tag{4}$$
$$x\bar{U}(x) = A_{\bar{U}}x^{B_{\bar{U}}}(1-x)^{C_{\bar{U}}}, \tag{5}$$
$$x\bar{D}(x) = A_{\bar{D}}x^{B_{\bar{D}}}(1-x)^{C_{\bar{D}}}, \tag{6}$$
$$xg(x) = A_g x^{B_g}(1-x)^{C_g}(1 + E_g x^2), \tag{7}$$
$$x\gamma(x) = A_\gamma x^{B_\gamma}(1-x)^{C_\gamma}(1 + D_\gamma x + E_\gamma x^2) \tag{8}$$
$$\tag{9}$$

The parametrisation for HERA data differs from that of the HERAPDF2.0 PDF since the starting scale Q_0^2 is higher and the additional negative term in the gluon parametrisation is not necessary. Parametrisation and model uncertainties are considered according to the HERAPDF procedure [**?**] by adding extra terms which make little difference to the χ^2 of the fit, but which can change the shape of the PDFs. Additonal parameters considered are: the extra negative term for the gluon; D_{u_v}, $D_{\bar{u}}$ and $E_{\bar{d}}$. Model variations considered are the variation of: m_b from 4.25 to 4.75 GeV; m_c from 1.41 to 1.53 GeV; Q_0^2 up to 10 GeV^2; Q_{cut}^2 up to 10 GeV^2; the strangeness fraction down to $f_s = 0.4$; the value of $\alpha_s(M_Z)$ from 0.116 to 0.120.

Fig. 1 shows the PDF distributions $x_{u_v}, xd_{d_v}, x\bar{u}, x\bar{d}, xg$ at $Q^2 = 7.5^2$ GeV^2, including model and parametrisation uncertainties, while Fig. 2 shows them at $Q^2 = 10^4$ GeV^2. *Add model and parametrisation variations, Use NNLO MC central.* In these figures comparisons are made to the NNPDF3.0PDF set and the HERAPDF2.0 set. The shape of the xd_{u_v} distribution is close to that of HERAPDF2.0 because of the dominance of HERA data in the fit.

Fig. 3 shows the comparison between the high-mass Drell-Yan double differential distribution and the predictions. The χ^2 values for the high-mass Drell Yan data and the output parameters from NNLO fit can be found in Table. 4 and Table. 5 respectively.

The NNLO photon PDF distribution is shown both at the starting scale (7.5 GeV^2) and at 10^4 GeV^2 in Fig. 6, where it is also compared to an NLO extraction of the photon distribution. The x-range of the figure is restricted to the range of sensitivity of the high-mass drell-Yan data; $0.045 < x < 0.35$. The NLO and NNLO photon PDFs are compatible over this range.

Fig. 7 shows the photon distribution in the restricted range compared to the NNPDF3.0qed NNLO photon PDF. The uncertainties are considerably reduced. The comparison is shown at scale 100 GeV^2 and at 10^4 GeV^2, where the value of 100 GeV^2 is chosen such that comparisons can also be made to the LUXqed [**?**] photon PDF, which is only defined above this scale. The HKR photon PDF [**?**] is also shown in this figure. The fit predictions from the present analysis agree with the LUXqed and the HKR photon PDFs at the 1-σ level.

V. CONCLUSIONS

In this work, ...

Appendix A: NLO QED corrections in APFEL

In this appendix we provide a detailed description of the implementation and validation of NLO QED corrections in `APFEL`. These can be separated into two main developments: first of all, the implementation of NLO corrections in the QED coupling α to the PDF evolution via the DGLAP evolution equations; secondly, the implementation of NLO QED coefficient functions for deep-inelastic structure functions. We now discuss these two improvements in turn.

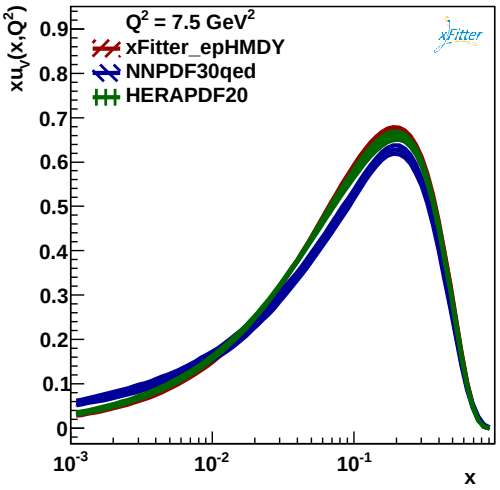
Q^2 = 7.5 GeV^2
xFitter_epHMDY
NNPDF30qed
HERAPDF20
xFitter
$xu_v(x,Q^2)$
x

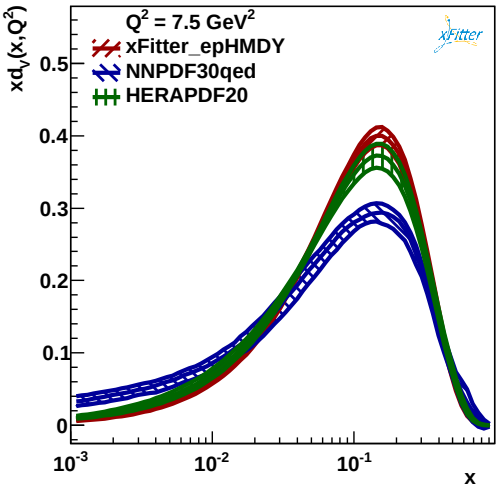
Q^2 = 7.5 GeV^2
xFitter_epHMDY
NNPDF30qed
HERAPDF20
xFitter
$xd_v(x,Q^2)$
x

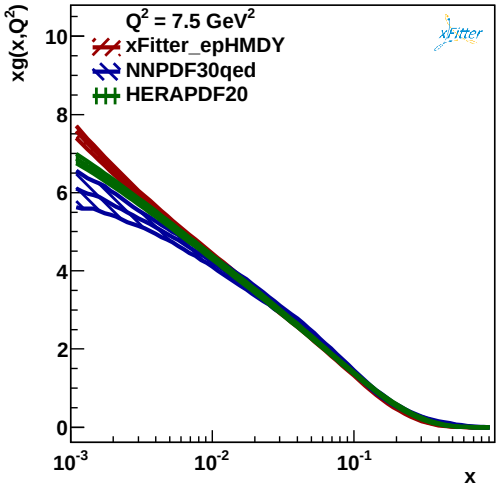
Q^2 = 7.5 GeV^2
xFitter_epHMDY
NNPDF30qed
HERAPDF20
xFitter
$xg(x,Q^2)$
x

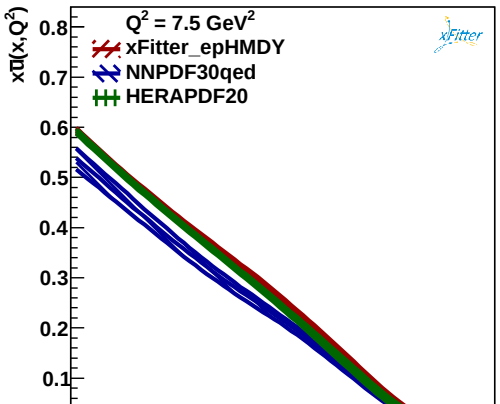
Q^2 = 7.5 GeV^2
xFitter_epHMDY
NNPDF30qed
HERAPDF20
xFitter
$x\bar{U}(x,Q^2)$

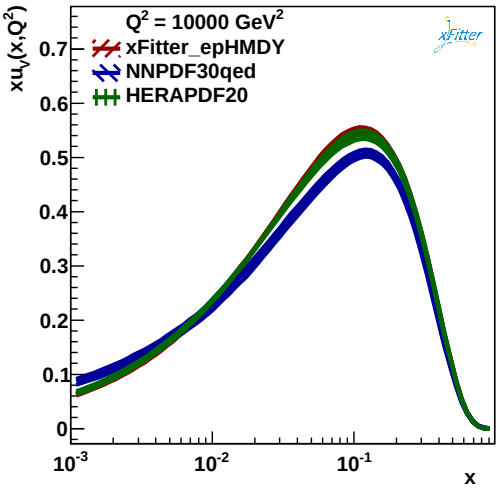
Q^2 = 10000 GeV^2
xFitter_epHMDY
NNPDF30qed
HERAPDF20
xFitter
$xu_v(x,Q^2)$
0.7
0.6
0.5
0.4
0.3
0.2
0.1
0
10^{-3}
10^{-2}
10^{-1}
x

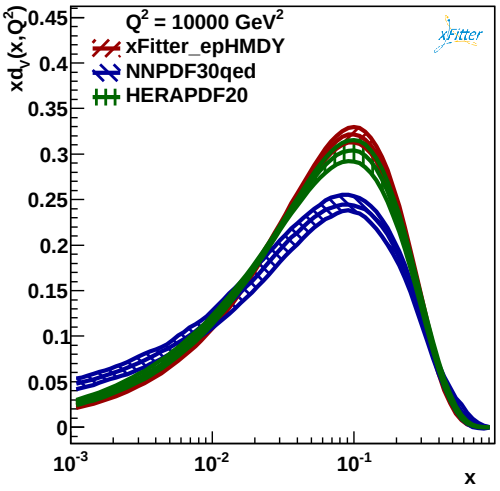
Q^2 = 10000 GeV^2
xFitter_epHMDY
NNPDF30qed
HERAPDF20
xFitter
$xd_v(x,Q^2)$
0.45
0.4
0.35
0.3
0.25
0.2
0.15
0.1
0.05
0
10^{-3}
10^{-2}
10^{-1}
x

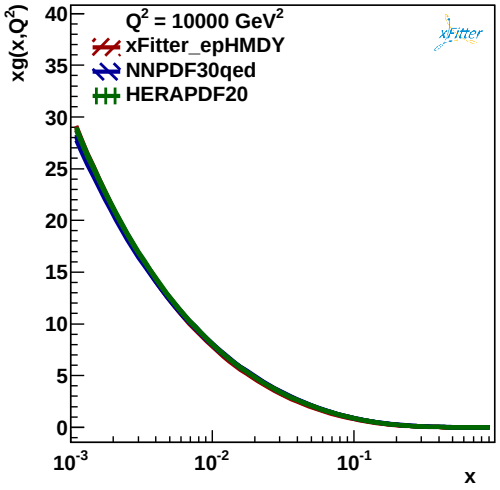
Q^2 = 10000 GeV^2
xFitter_epHMDY
NNPDF30qed
HERAPDF20
xFitter
$xg(x,Q^2)$
40
35
30
25
20
15
10
5
0
10^{-3}
10^{-2}
10^{-1}
x

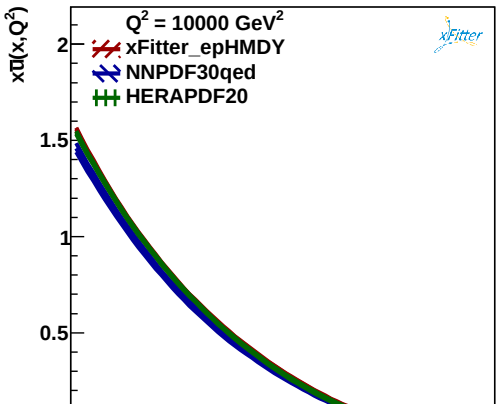
Q^2 = 10000 GeV^2
xFitter_epHMDY
NNPDF30qed
HERAPDF20
xFitter
$x\bar{U}(x,Q^2)$
2
1.5
1
0.5

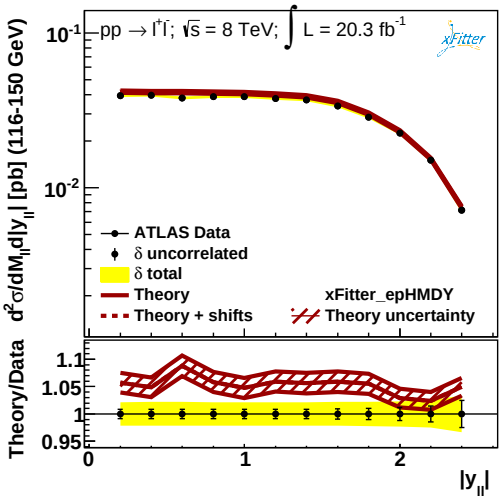
pp → l⁺l⁻; √s = 8 TeV; ∫ L = 20.3 fb⁻¹
xFitter
ATLAS Data
δ uncorrelated
δ total
Theory
Theory + shifts
xFitter_epHMDY
Theory uncertainty
d²σ/dM_ll dy_ll [pb] (116-150 GeV)
Theory/Data
|y_ll|

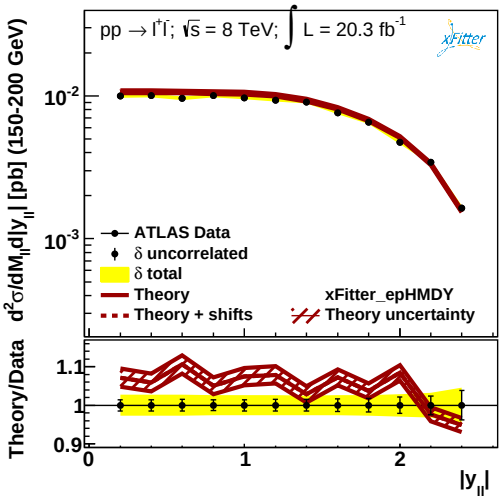
pp → l⁺l⁻; √s = 8 TeV; ∫ L = 20.3 fb⁻¹
xFitter
ATLAS Data
δ uncorrelated
δ total
Theory
Theory + shifts
xFitter_epHMDY
Theory uncertainty
d²σ/dM_ll dy_ll [pb] (150-200 GeV)
Theory/Data
|y_ll|

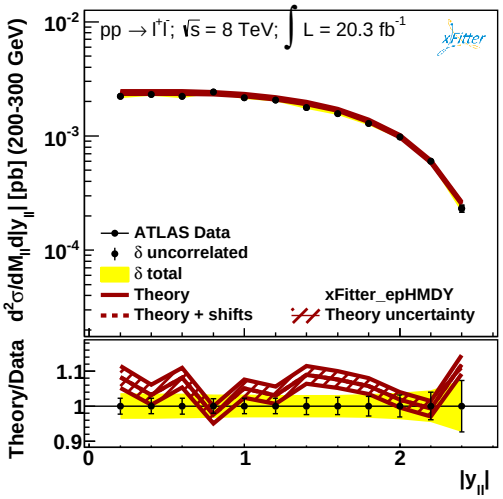
pp → l⁺l⁻; √s = 8 TeV; ∫ L = 20.3 fb⁻¹
xFitter
ATLAS Data
δ uncorrelated
δ total
Theory
Theory + shifts
xFitter_epHMDY
Theory uncertainty
d²σ/dM_ll dy_ll [pb] (200-300 GeV)
Theory/Data
|y_ll|

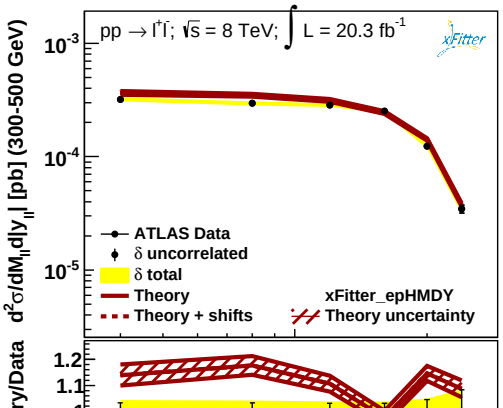
pp → l⁺l⁻; √s = 8 TeV; ∫ L = 20.3 fb⁻¹
xFitter
ATLAS Data
δ uncorrelated
δ total
Theory
Theory + shifts
xFitter_epHMDY
Theory uncertainty
d²σ/dM_ll dy_ll [pb] (300-500 GeV)
Theory/Data

Dataset	xFitter epHMDY
HMDY rap 116-150	9.3 / 12
HMDY rap 150 200	17 / 12
HMDY rap 200 300	15 / 12
HMDY rap 300 500	3.8 / 6
HMDY rap 500 1500	4.2 / 6
Correlated χ^2	4.98
Log penalty χ^2	-3.64E-04
Total χ^2 / dof	55 / 48
χ^2 p-value	0.01

Figure 4. χ^2 for high-mass Drell Yan data, for the NNLO fit

Parameter	xFitter epHMDY
'Bg'	$-0.220^{+0.014}_{-0.013}$
'Cg'	$6.92^{+0.62}_{-0.61}$
'Buv'	$0.761^{+0.017}_{-0.015}$
'Cuv'	$5.060^{+0.064}_{-0.092}$
'Euv'	$8.07^{+0.80}_{-0.82}$
'Bdv'	$1.009^{+0.050}_{-0.056}$
'Cdv'	$5.61^{+0.24}_{-0.30}$
'Cubar'	$6.37^{+0.56}_{-0.38}$
'Adbar'	$0.3226^{+0.0078}_{-0.0083}$
'Bdbar'	$-0.1921^{+0.0033}_{-0.0033}$
'Cdbar'	$14.0^{+2.0}_{-1.7}$
'alphas'	0.1180
'rs'	1.0000
'Aph'	$0.00120^{+0.031}_{-0.00089}$
'Bph'	$-0.62^{+0.63}_{-0.36}$
'Cph'	$10.0^{+13}_{-5.9}$
'Dph'	-4^{+210}_{-15}
'Eph'	87^{+257}_{-140}
Fit status	MC-replica
Uncertainties	median±68cl

Figure 5. PDF parameters for the NNLO fit.

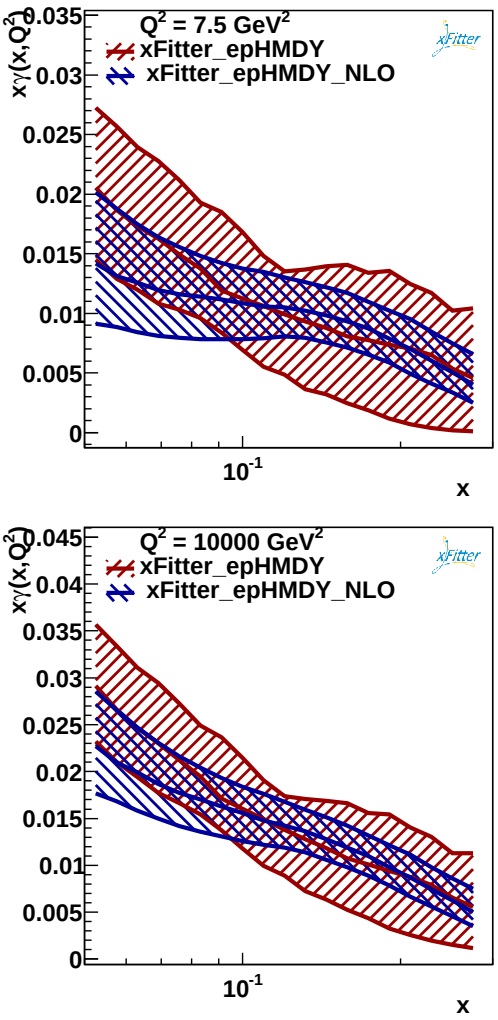

Figure 6. Comparison between the photon PDF distributions at NNLO and NLO: (a) at the starting scale; (b) at the evolved scale.

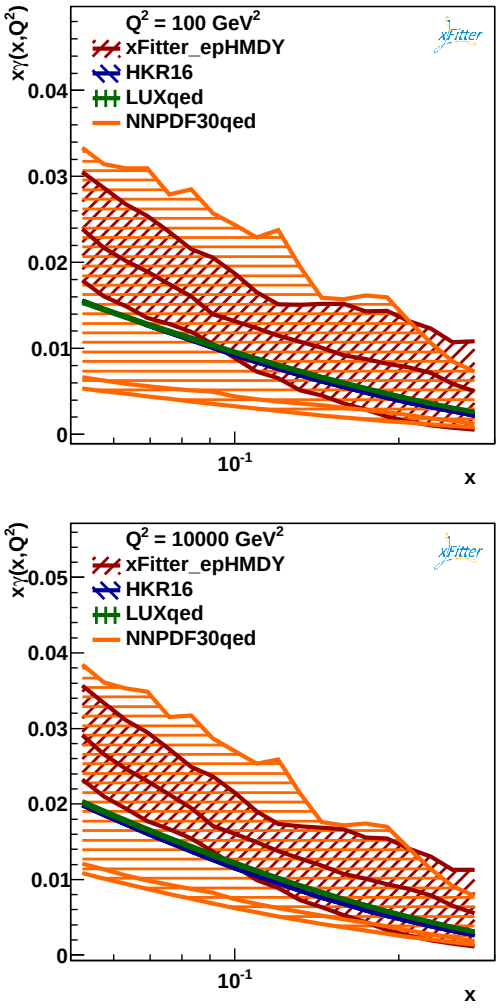

Figure 7. Comparison between the NNLO photon PDF distributions for the present analysis, NNPDF3.0QED, LUXqed, HKR: (a) at scale 100 GeV^2; (b) at the evolved scale 10000 GeV^2.